Formation of Self-Supporting Reversible Cellular Networks in Suspensions of Colloids and Liquid Crystals

Doris Vollmer,*,† Gerald Hinze,‡ Beate Ullrich,† Wilson C. K. Poon,§,|| Michael E. Cates,§ and Andrew B. Schofield§

MPI for Polymer Research, Ackermannweg 10, 55128 Mainz, Germany, Institute for Physical Chemistry, Jakob-Welderweg 11, 55099 Mainz, Germany, and School of Physics and Collaborative Optical Spectroscopy, Micromanipulation and Imaging Centre (COSMIC), The University of Edinburgh, JCMB, Kings Buildings, Mayfield Road, Edinburgh EH9 3JZ, United Kingdom

Received November 26, 2004. In Final Form: March 10, 2005

In mixtures of thermotropic liquid crystals with spherical poly (methyl methacrylate) particles, self-supporting networklike structures are formed during slow cooling past the isotropic-to-nematic phase transformation. To characterize the process of network formation in terms of morphology, phase transformation kinetics, and mechanical properties, we have combined data from polarization and laser scanning confocal microscopy with calorimetric, NMR, and rheological results. Our data suggest that the mechanism of network formation is dominated by a broadened temperature and time interval of phase transformation rather than by particle size or concentration. The observation that the width of the transformation interval strongly depends on sample preparation supports the hypothesis that a third component, most likely alkane remnants slowly liberated from the particles, plays a crucial role. In addition, calorimetric findings for liquid crystal/colloid mixtures, heated and cooled up to 13 times, point to separation of the liquid crystal into two compartments with different phase transformation kinetics. This could be explained by redistribution and enrichment of alkane in the particle-composed network walls. A further increase of the storage modulus, G', and incomplete dissolution of the networks in the isotropic state indicate that the formation of two compartments during repeated temperature cycles stabilizes the network and confers strong memory effects.

I. Introduction

Liquid crystals have been studied intensively as they are model systems for anisotropic fluids with adjustable properties.[1−4] Colloids are widely used to model hard spheres or particles with tunable interactions.[5−8] Both systems exhibit a rich variety of phases, caused by an interplay of energies of different origin but similar magnitude.

However, so far little is known about the interactions of thermotropic liquid crystal and colloids in mixtures, that is, colloids suspended in an anisotropic solvent.[9,10] In general, mixtures of two phase-forming components often show a strong tendency to demix, or an even richer phase behavior is observed than in the individual components. This includes novel phases with unexpected structures and macroscopic properties.

In mixtures of liquid crystal with colloidal particles or droplets, the latter both tend to be expelled from the nematic phase due to its long-range orientational elasticity. Recently it has been shown that this microscopic phase separation can generate structural patterns of long-term stability whose morphological features depend on the experimental protocol and on the nature of the particles added:[11−14]

(i) In mixtures of liquid crystal with small amounts of an isotropic liquid, phase separation may induce self-organization of isotropic liquid droplets into highly ordered chains.[11−13]

(ii) In suspensions of sterically stabilized colloidal particles dispersed in liquid crystal, self-supporting cellular structures are observed after cooling through the isotropic-to-nematic transformation.[14−16]

To gain insight into the differences between both systems it should be noted that in system (i) a binary mixture is either *quenched* from the isotropic into the nematic phase or homogenized in the nematic phase. However, because in the nematic phase both liquids are immiscible, phase separation causes nucleation and

† MPI for Polymer Research.

‡ Institute for Physical Chemistry.

§ School of Physics, The University of Edinburgh.

|| Collaborative Optical Spectroscopy, Micromanipulation and Imaging Centre (COSMIC), The University of Edinburgh.

(1) de Gennes, P. G.; Prost, J. *Physics of Liquid Crystals*; Clarendon: Oxford, 1993.

(2) Crawford, G. P.; Zumer, S. *Liquid Crystals in Complex Geometries*; Taylor and Francis: London, 1996.

(3) Fraden, S. In *Observation, Prediction, and Simulation of Phase Transitions in Complex Fluids*; Baus, M., Rull, L. F., Ryckaert, J. P., Eds.; Kluwer Academic: Dordrecht, 1995; pp 113−164.

(4) Onsager, L. *Ann. N.Y. Acad. Sci.* **1949**, *51*, 627.

(5) Pusey, P. N. In *Liquids, Freezing and the Glass Transition*; Hansen, J. P., Levesque, D., Zinn-Justin, J., Eds.; NATO Advanced Study Institute at Les Houches; North-Holland: Amsterdam, 1991; pp 763−942.

(6) Anderson, V. J.; Lekkerkerker, H. N. W. *Nature* **2002**, *416*, 811.

(7) Yethiraj, A.; von Blaaderen, A. *Nature* **2003**, *421*, 513.

(8) Frenkel, D. In *Liquids, Freezing and the Glass Transition*; Hansen, J. P., Levesque, D., Zinn-Justin, J., Eds.; Elsevier Science: Amsterdam, 1991; Ch. 9, pp 689−762.

(9) Terentjev, E. M. *Phys. Rev. E* **1995**, *51*, 1330.

(10) Kuksenok, O. V.; Ruhwandl, R. W.; Shiyanovskii, S. V.; Terentjev, E. M. *Phys. Rev. E* **1996**, *54*, 5198.

(11) Poulin, P.; Stark, H.; Lubensky, T. C.; Weitz, D. A. *Science* **1997**, *275*, 1770.

(12) Poulin, P.; Weitz, D. A. *Phys. Rev. E* **1998**, *57*, 626.

(13) Loudet, J.-C.; Barois, P.; Poulin, P. *Nature* **2000**, *407*, 611.

(14) Meeker, S. P.; Poon, W. C. K.; Crain, J.; Terentjev, E. M. *Phys. Rev. E* **2000**, *61*, R60836.

(15) Vollmer, D.; Hinze, G.; Poon, W. C. K.; Cleaver, J.; Cates, M. E. *J. Phys.: Condens. Matter* **2004**, *16*, L227.

(16) Anderson, V. J.; Terentjev, E. M.; Meeker, S. P.; Crain, J.; Poon, W. C. K. *Eur. Phys. J. E* **2001**, *4*, 11.

(17) Anderson, V. J.; Terentjev, E. M. *Eur. Phys. J. E* **2001**, *4*, 21.

10.1021/la047090w CCC: $30.25
Published on Web 04/21/2005

growth of droplets. At a critical droplet size (typically a few micrometers), coarsening stops and the droplets form long chains aligned parallel to the director. Chain formation could be explained by the interplay of the energy specifying a deviation from the preferential orientation of the liquid crystal at the liquid crystal/colloid interface (WR^2) and the bulk orientational elasticity of the liquid crystal (KR), where W denotes a surface energy term, K is the elastic constant (assumed to be equal for splay, twist, and bend deformations), and R is the radius of the particles. For large particles, $R > K/W$, the surface energy becomes dominant (strong anchoring) and the liquid crystal preserves its preferred orientation at the surface (in the investigated case a normal orientation), leading to chaining of droplets.[18]

This mechanism of microscopic phase separation must be contrasted with the mechanism in system (ii), where the kinetics of phase separation under *slow cooling* is relevant. In this case, the formation of a three-dimensional network is observed. Because the first studies have been performed with ≈200-nm-sized particles, it was expected that network formation could be related to the weak anchoring limit ($R < K/W$).[14,16,17]

The present study was performed to shed more light onto the microscopic and macroscopic feature of network formation. Only recently[15,19] it has been shown that network formation may also be observed for micrometer-sized particles and that previous studies[14,16,17] have not been dealing with binary but with *ternary* systems.[20] Alkane remnants resulting from particle preparation cannot be removed completely but slowly diffuse into the suspension after homogenization. Alkane can interfere with particle rearrangement in two ways: First, wetting of the particles either by isotropic material or by a layer of alkane will alter the anchoring of the liquid crystal molecules on the particle surface. Second, in the presence of alkane the temperature of the isotropic/nematic phase transformation is lowered and a biphasic region shows up.[21,22] Isotropic and nematic phases coexist for the duration of the phase transformation. Because particle networks are formed during this time interval, it seems to be critical that the system remains biphasic for a sufficient period of time.

Data from polarization and confocal microscopy, calorimetry, nuclear magnetic resonance (NMR), and rheology have been combined to correlate the temperature-dependent change of the fraction of isotropic and nematic material as measured by NMR with phase transformation kinetics, particle movement, and colloidal network stability. Microscopically, both the movement of individual particles and the assembly of structures could be followed (sections III.A and III.B). Because it was not clear whether eventually all of the solvent reaches the nematic state or if submicroscopic isotropic domains are left far below the calorimetrically and optically determined transformation temperature, NMR was used to estimate the fractions of isotropic and nematic material as a function of temperature (sections III.C and III.D). Network formation is also reflected in temperature-dependent changes of loss and storage moduli (section III.E). In section IV we studied the reversibility of particle network formation during repeated heating/cooling. Typical constraints and possible artifacts are discussed (section VII). The paper is concluded with a discussion of the results in section V.

II. Experimental Section

A. Sample Preparation. Poly(methyl methacrylate) particles (PMMA) with radii of 100−1000 nm sterically stabilized by chemically grafted poly(12-hydroxy-stearic acid) molecules ≈15 nm in length[23,24] were dispersed in 4-*n*-pentyl-4′-cyanobiphenyl (5CB; Merck, used as supplied). For laser scanning confocal microscopy (LSCM), PMMA particles were labeled using fluorescent monomers (7-nitrobenzo-2-oxa-1,3-diazol-methyl-methacrylate)[25] which was chemically attached to PMMA. The radii were determined either from diffusion coefficients or lattice parameters in the crystal phase of colloids. The former measurements also gave a polydispersity of <0.1 (except for particles with $R \geq 700$ nm for which it was not measured). Unless otherwise stated, the particles, initially dispersed in heptane or hexane, were dried in a vacuum oven (≈10^{-2} mbar) at 45 °C for up to 1 week, then dispersed in 5CB, and homogenized in the isotropic phase for several weeks. The suspensions were continuously stirred at 45 °C until just before use. Calorimetry gave a phase transition temperature [IMAGE] = 35.2 °C for bulk 5CB.

B. Optical Microscopy. Just before use, a defined amount of hexane was added to the samples, typically between 0.1 and 2 vol %. Subsequently, 50 μL of each mixture was pipetted onto a preheated quartz tray (Linkam, U.K.). Samples were placed on a Linkam THMS-600 heating stage, kept at 60 °C for 10 min, and cooled to 36 °C at −300 K/h and then to 30 °C at a rate of −3 K/h. Temperature was controlled and monitored with a Linkam TMS 94 unit with an accuracy of 0.1 K. Counter-cooling was done using a Linkam LNP with room air (20 °C) as a coolant. The samples were viewed under an Olympus BX51 microscope in transmitted light, using a 100× long distance objective. In the heating stage used, the temperature sensor is placed within the metal heating block whereas the sample is observed through an opening in the middle sealed with glass. For this reason the recorded phase transformation temperatures were consistently ≈0.3 K higher than those found in calorimetry. Images were taken with an Evolution MP5 camera (Qimaging, Canada) every 2 s, corresponding to an average temperature change of 0.0017 K.

C. LSCM. In suspensions with higher particle concentrations (>10 wt %), we investigated the morphology of colloidal network formation by LSCM. About 0.05 mL of suspension was loaded into a homemade sample holder sealed on the lower end with a coverslip. The sample holder consisted of a metal heating block, shaped like a truncated cone of 5 mm height and a smaller diameter of 3 mm. These dimensions significantly reduced wall artifacts encountered in previous investigations.[26] Because of the high sensitivity of the detector (single-photon avalanche photodiode), a laser ($\lambda = 488$ nm) power of 2 nW was sufficient to resolve the fluorescent particles. This low laser power reduces photobleaching of the dye molecules, permitting particle tracking for several days.

The temperature of the copper heating block was measured with a platinum thermocouple. Close to the coverslip the temperature was slightly lower than inside the metal vessel. Calibration with samples of known temperature yielded an accuracy of ≈0.5 K. However, relative values of the temperature could be determined with an accuracy of 0.01 K (Lakeshore, temperature controller). A cooling/heating rate of 6 K/h was chosen, and images were taken every 100 s.

D. Calorimetry. The specific heat was measured using a differential scanning microcalorimeter (VP-DSC, Microcal, Inc.).[27]

(18) Stark, H. *Phys. Rep.* **2001**, *351*, 387.
(19) Cleaver, J.; Poon, W. C. K. *J. Phys.: Condens. Matter* **2004**, *16*, S1901.
(20) Because the particles investigated in refs 14, 16, 17, and 35 were prepared and handeled according to the same procedure, all samples contained a small amount of alkane.[15]
(21) Oweimreen, G. A.; Martire, D. E. *J. Chem. Phys* **1980**, *72*, 2500.
(22) Orendio, H.; Ballauff, M. *Ber. Bunsen-Ges. Phys. Chem.* **1991**, *96*, 96.
(23) Antl, L.; Goodwin, J. W.; Hill, R. D.; Ottewill, R. H.; Owens, S. M.; Papworth, S.; Waters, J. A. *Colloids Surf.* **1986**, *17*, 67.
(24) Bosma, G.; Pathmamanoharan, C.; de Hoog, E. H. A.; Kegel, W. K.; van Blaaderen, A.; Lekkerkerker, H. N. W. *J. Colloid Interface Sci.* **2002**, *245*, 292.
(25) Jardine, R. S.; Bartlett, P. *Colloids Surf., A* **2002**, *211*, 127. Jardine, R. S. Ph.D. Thesis, University of Bristol, Bristol, U.K., 2000.
(26) Cleaver, J.; Vollmer, D.; Crain, J.; Poon, W. C. K. *Mol. Cryst. Liq. Cryst.* **2004**, *409*, 59.
(27) Plotnikov, V. V.; Brandts, J. M.; Lin, L. N.; Brandts, J. F. *Anal. Biochem.* **1997**, *250*, 2237.

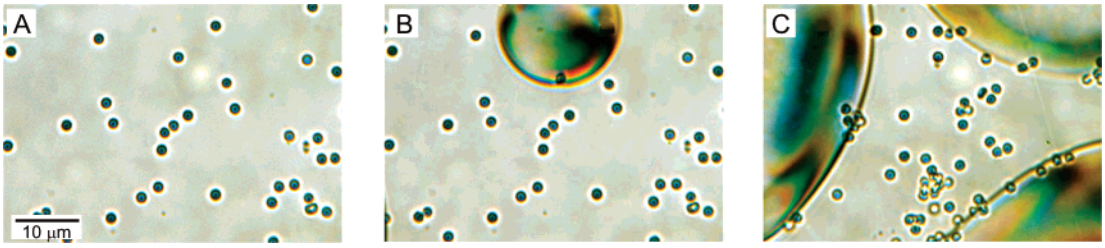

Figure 1. Images taken by polarization microscopy of a suspension containing 0.1% particles with a radius of 1 μm dispersed in a mixture of 5CB and 0.5% hexane. The images reflect the temperature-dependent arrangement of the particles, visible as dark spots surrounded by a light ring. (A) Just above entering the biphasic region, T_{IN}; (B) 2 s later, a nematic droplet appears in the upper part of the image; and (C) 32 s later, the particles are pushed together by the moving surfaces of three nematic droplets whose interior is devoid of particles.[29]

This microcalorimeter consists of two coin-shaped fixed-in-place twin cells of 0.52 cm^3 each. The sample cell is filled with the solution to be investigated, while the reference cell is filled with a mixture of comparable heat capacity that does not show any temperature-induced reactions or transitions within the temperature interval under investigation. In our case, a mixture of water and octane was used as a reference. Because only changes of specific heat as compared to the reference solution were measured, we refer to the values as $C_v^{rel}(T)$. The preheated sample cell was loaded with the homogenized suspension taking care that both the sample and the filling syringe were kept at a temperature well within the isotropic region during the filling procedure. If not explicitly stated, sample material was exchanged for every scan.

E. NMR. To investigate the fraction of isotropic material below the bulk nematic transition, we measured the temperature-dependent orientational order of the liquid crystal by ^{1}H NMR at 90 MHz.[28] A narrow, liquidlike peak in the NMR spectrum is characteristic for the isotropic phase. In the nematic phase, rotational anisotropy of the molecules leads to nonvanishing dipolar interactions, which are seen as a broad spectrum with a characteristic line splitting.[28] Other components with dynamics slower than the inverse line width ($<10^{-5}$ s) lead to Gaussian shaped broad spectra, which can be discriminated from the nematic phase. Spectra were recorded after applying a solid echo pulse sequence. Different relaxation times T_2 of the components were accounted for by varying the delay between the two pulses. Temperature was controlled by a Lakeshore temperature controller allowing for an accuracy of the absolute temperature of $\approx$0.2 K.

F. Rheology. The temperature dependence of the loss G'' and storage $G'(T)$ moduli was monitored using a rheometer (CSL^2-100, TA Instrument) set up in the cone-and-plate geometry with a cone diameter of 4 cm and an angle of 2° and operated in the oscillatory mode. Within experimental accuracy, no dependence on the cone radius and angle was observed. The measurements were done at a frequency of 1 Hz, unless stated otherwise. The maximal strain amplitude was chosen to be as small as possible and did not exceed 2%, unless stated otherwise. In oscillatory mode, for moduli above $\approx 5 \times 10^5$ Pa and below $\approx$1 Pa there are nonquantifiable systematic errors caused by the resolution of the rheometer. Because of thermal expansion of the cone and plate the distance between both increases by $\approx$1.5 μm per degree. The moduli are corrected for variation of the distance, assuming that it does not alter the structure of the sample. If not stated otherwise, homogenized samples were loaded into the rheometer taking care that the sample remained isotropic during loading. The samples were pre-sheared at 45 °C for 10 min at 50 Hz. The measurements were started 2 min after the end of the pre-shear.

III. Results

A. Optical microscopy. To characterize the localization of the particles during the isotropic-to-nematic transformation of the liquid crystal, we investigated a dilute suspension of particles ($\phi_{PMMA} = 0.1$ wt %) in 5CB and hexane ($\phi_{hex} = 0.5$ vol %) cooled at a rate of -3 K/h (see also ref 19). Until just above entering the biphasic region ($T \gtrsim T_{IN}$), the particles, visible as rings, were homogeneously distributed (see Figure 1A). Passing T_{IN}, birefringent nematic domains began to grow. Due to the presence of hexane, visible nematic/isotropic interfaces propagated with speeds low enough to be measured.[19,29,30] A nematic droplet entering the image area from above is shown in Figure 1B. The nematic droplets were essentially devoid of particles. The PMMA particles, having a higher affinity to the isotropic than to the nematic phase, were pushed ahead by the moving interface, leading to enrichment of particles in the isotropic domains (Figure 1A,C).

B. LSCM. In suspensions with higher particle concentrations, we investigated network formation by LSCM (see also refs 19 and 26). The temperature-dependent structure of a suspension of 15% PMMA particles (R = 204 nm) dispersed in 5CB and cooled with a rate of -6 K/h is depicted in Figure 2. Position- and temperature-dependent changes of local particle concentration are reflected by the intensity of fluorescence. After loading the sample in the isotropic phase (T = 45 °C), particles were arranged homogeneously. Just before the phase transformation, only small variations of the average particle concentration were noticeable Figure 2A. Entering the biphasic region gave rise to the formation of particle-free nematic droplets surrounded by particle-rich domains (B). During further cooling, rearrangement, nucleation, and growth of bubble-shaped nematic domains were observed. Particles were swept together until a dense particle network emerged filling the space between the nematic droplets. While rearrangement within the network was going on (until $\approx$1.5 K below T_{IN}; see Figure 2B$-$G) the structure was very fragile and sensitive to external perturbations. At about 1.5 K below T_{IN} (i.e., after 15 min) particle and droplet rearrangement almost ceased (G) and the structure froze (H). After longer intervals in the nematic phase, occasionally cracks appeared in thin particle walls, forming connections between neighboring liquid crystal-filled cavities.

In LSCM of networks wall artifacts and decreased resolution with increasing imaging depth constitute major problems. In our experiments the image plane was chosen 10 μm above the coverslip, that is, 25 particle diameters. Therefore, particle distribution and movement during the initial stage of the phase transition reflect bulk behavior, whereas wall artifacts become relevant as soon as the cavity diameter exceeds 10 μm. Therefore, the final shape of the cells as shown in Figure 2F$-$H may not reflect the bulk structure. However, LSCM imaging at a depth of

(28) Dong, R. Y. *Nuclear magnetic resonance of liquid crystals*; Springer: New York, 1994.

(29) West, J. L.; Glushchenko, A.; Liao, G.; Reznikov, Y.; Andrienko, D.; Allen, M. P. *Phys. Rev. E* **2002**, *66*, 012702.

(30) In contrast, the phase transition is instantaneous in pure 5CB. Trace impurities, however, can lead to finite speeds as observed in ref 19.

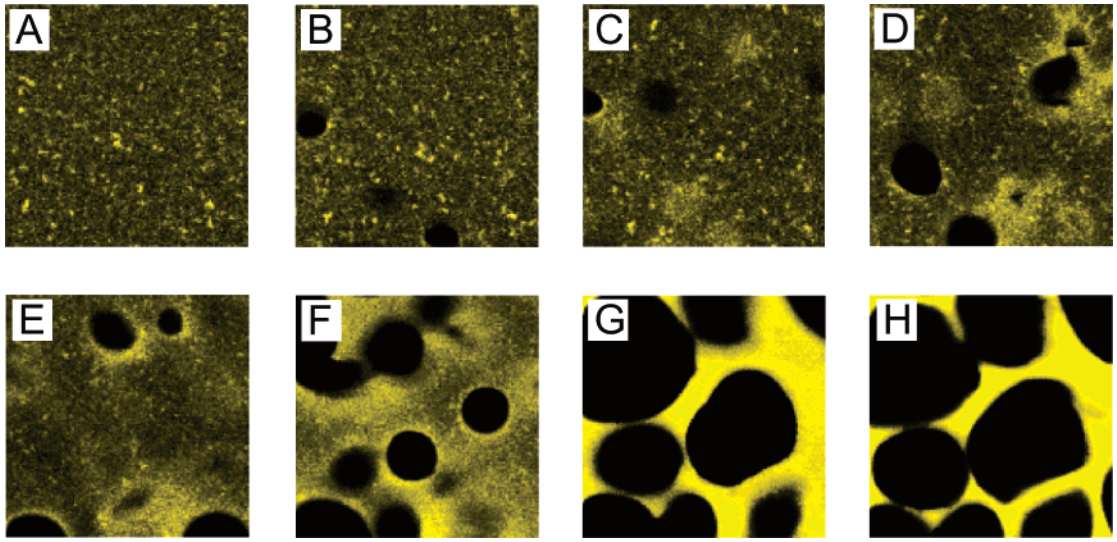

Figure 2. Images of a sample containing 15 wt % fluorescent PMMA particles ($R = 204$ nm) dispersed in 5CB. The particles are shown in yellow, whereas the liquid crystal appears black. The sample was loaded in the isotropic phase and cooled with a rate of −6 K/h from 45 to 25 °C. Images were taken 10 μm beyond the coverslip every 100 s. They reflect the structure of the sample at temperatures (A) 33.38 °C; (B) 33.25 °C; (C) 33.13 °C; (D) 33.00 °C; (E) 32.75 °C; (F) 32.50 °C; (G) 31.75 °C; and (H) 25 °C. Confocal area: 80 × 80 μm^2.

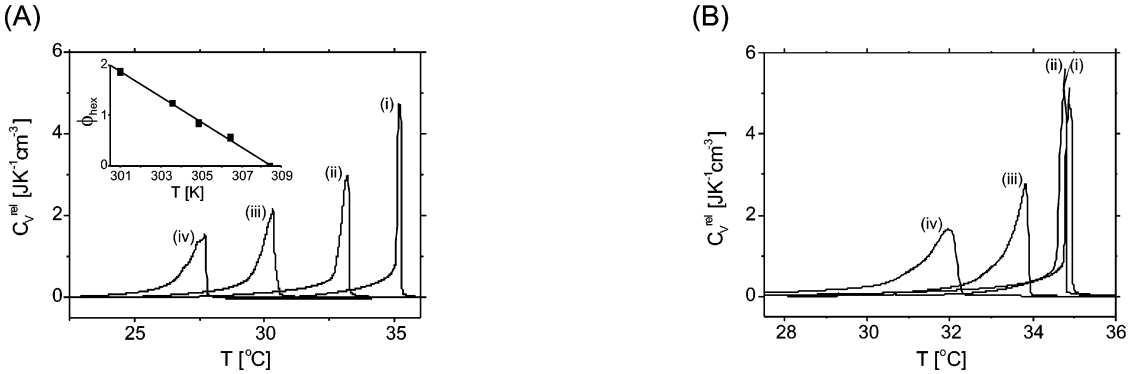

Figure 3. (A) Dependence of the specific heat C_v^{rel} on temperature in mixtures of 5CB with hexane. (i) Pure 5CB; (ii) 0.6 wt %; (iii) 1.3 wt %; and (iv) 1.9 wt % hexane in 5CB. Cooling rate: ≈−4 K/h. Inset: dependence of the phase transformation temperature [IMAGE] on the weight fraction of hexane ϕ_{hex}. T_{IN} is defined by a sharp rise of the heat peak. The transition temperature linearly decreases with increasing hexane concentration. (B) Dependence of the specific heat C_v^{rel} on temperature in 5CB/particle mixtures with different pretreatments. (i) Pure 5CB; (ii) 10 wt % of intensively dried PMMA in 5CB, $R = 430$ nm, measured 1 week after preparation; (iii) intensively dried PMMA in 5CB after stirring the sample for 7 weeks; and (iv) typical drying procedure and stirring the suspension for about 6 weeks, 10 wt % PMMA in 5CB, $R = 430$ nm. Cooling rate: ≈−4 K/h.

several times the cavity size is not possible due to poor resolution. Nevertheless, the images illustrate the characteristic pattern and time scales of network formation.[31]

C. Microcalorimetry. To test whether the presence of alkane, especially hexane, impurities are responsible for the broadening of the phase transformation[15] we investigated mixtures of 5CB and hexane, as well as suspensions of 5CB and colloids, by microcalorimetry. The appearance of a biphasic region is reflected in the temperature dependence of specific heat $C_v^{rel}(T)$. The thermograms of samples containing 5CB and different amounts of hexane are shown in Figure 3A. In a one-component system the phase transition should cause a peak of vanishing width in the specific heat. Figure 3A(i) shows the thermogram of "pure" 5CB (i.e., 5CB as supplied by the manufacturer). Its finite width shows that even "pure" 5CB contains a certain amount of impurities. According to the manufacturer, this broadening is most likely due to trace amounts of nematogen with different chain lengths. Adding hexane caused a reduction of the phase transformation temperature and a further increase of the width of the peak in C_v^{rel} [Figure 3A(ii−iv). According to ref 21, it should not exceed 5 K for the concentrations investigated. However, in mixtures with PMMA particles, we find changes significantly in excess of this figure. In line with expectations[21,22] a linear decrease of T_{IN} was observed, given by

$$T_{IN} = [308.4 - (4.0 \pm 0.3)\phi_{hex}]K \qquad (1)$$

where ϕ_{hex} denotes the weight percent of hexane (inset). In these experiments, it could not be determined where the heat curves meet the baseline. Thus, there is some uncertainty in measuring the precise width of the peak.

The thermograms of particle−5CB suspensions in Figure 3B strikingly resemble those of mixtures of 5CB with hexane in Figure 3A. The thermograms in Figure 3B(ii−iv) depict the influence of the treatment of the particles, while the radius of the particles ($R = 460$ nm) and concentration of particles (10 wt %) were kept fixed.

(31) The images shown in ref 19 were taken in 300-μm-thick capillaries 100 μm above the bottom plane. According to the images the domain size can exceed 250 μm. In that case no three-dimensional bulk structure can evolve, because the cavities may span almost the entire thickness of the capillary.

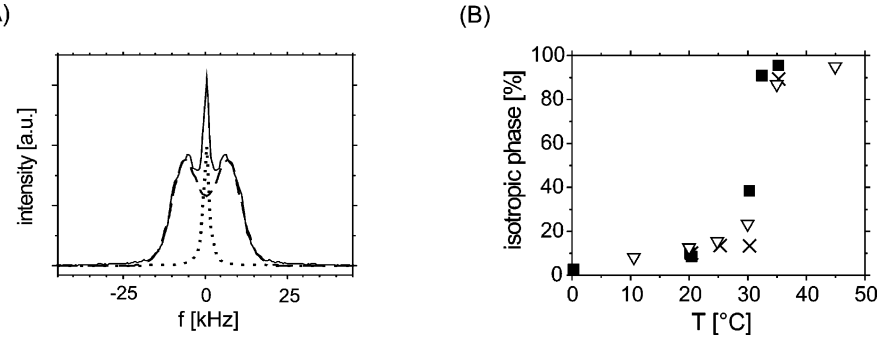

Figure 4. (A) ^{1}H NMR solid echo spectrum, taken at 30 °C. Particle size: $R = 430$ nm. Solid line, spectrum of the sample; dotted line, fit of the isotropic fraction; dashed line, fit of the nematic fraction. (B) Temperature dependence of the fraction of the isotropic phase for different particle sizes. ■, $R = 120$ nm; ▽, $R = 430$ nm; ×, $R = 780$ nm. Weight fraction of colloids: 15%.

For comparison a thermogram of pure 5CB, Figure 3B(i), is also presented. Particles dried at ≈60 °C and ≈10^{-5} mbar, mixed with 5CB, and stirred for 1 week gave a thermogram [Figure 3B(ii)] with a peak width and position similar to those of pure 5CB [Figure 3(i)] but at a slightly lower temperature. Stirring the sample for another 6 weeks yielded a further decrease of T_{IN} and a broadening of the peak; see Figure 3B(iii). This points to slow liberation of alkane molecules, presumably because they are trapped not only in the hairs (polymerized 12-hydroxy-stearic acid linked to the particle surface for steric stabilization) but also in the core of the particles. It is also possible that besides or in addition to alkanes, tiny amounts of unreacted monomers could slowly be released into the medium.[32] Less intensive drying of the particles (≈45 °C and ≈10^{-2} mbar) gave rise to thermogram (iv) in Figure 3B, with an even lower transformation temperature and a further increase of the width of the biphasic region.

D. NMR. The above results raise the question how far below T_{IN} isotropic material is still detectable and when the phase transformation is completed. The fraction of isotropic compared to nematic material can be estimated in PMMA/5CB mixtures from the shape of the NMR spectrum. A typical ^{1}H spectrum is given in Figure 4a for a suspension of 15% PMMA particles ($R = 430$ nm) dispersed in 5CB. The spectrum is a superposition of a narrow peak corresponding to the isotropic phase, superimposed on a broader peak that reflects the nematic phase. The splitting of this component (Figure 4) is well-known. Each spectrum was fitted to a narrow Lorentzian peak and a broader Pake-like spectrum.[28] Different t_2 relaxations of the two components were accounted for by measuring several spectra depending on the pulse distance of the solid-echo pulse sequence and subsequent extrapolation to $dt \rightarrow 0$. While below the phase transformation temperatures this evaluation works well, at higher temperatures $T \approx T_{IN}$ the fraction of the nematic phase decreases significantly. Here the quantitative composition of the NMR signal was analyzed from the time domain data instead of the spectra. In Figure 4b the volume fraction of the isotropic phase is shown for three different samples.

A wide transition region was found for all three particle sizes investigated ($R = 120$ nm, $R = 430$ nm, and $R = 780$ nm). Even 10 K below T_{IN} ($T_{IN} \approx 32°$), isotropic material accounted for >10% of the signal. This is surprising, because in mixtures of liquid crystal and hexane the biphasic region is expected to be smaller than 5 K for hexane concentrations less than a few percent. A possible explanation is that local hexane concentrations may change considerably during and after phase transformations. According to Figure 1C, the particles obviously have a higher affinity to the isotropic than to the nematic phase. Assuming that the particles are wetted by solvent enriched in hexane, this would lead to enrichment of hexane in the particle-rich domains (and to depletion in the network cavities), resulting in local hexane concentrations much higher than expected according to eq 1. However, we were not able to determine the local hexane concentrations quantitatively. Furthermore, liberation of tiny amounts of unreacted monomer may add to increase of the width of the biphasic region; however, we expect this effect to be of minor relevance.

E. Rheology. To study the mechanical stability of the network we measured the temperature dependence of the loss $G''(T)$ and the storage G' moduli for particle sizes between 100 and 780 nm and particle concentrations of 5, 10, and 15 wt %. Samples were cooled in situ at rates between −3 and −10 K/h at a fixed frequency of $f = 1$ Hz.

As an example $G''(T)$ is shown for a sample containing 10 wt % of particles, Figure 5A: At $T \approx 33.5$ °C, $G''(T)$ starts to increase until it takes values of $(3 \pm 2) \times 10^5$ Pa close to 20 °C. In contrast, $G''(T)$ for pure 5CB (dashed line) depends only weakly on temperature.[33] In the isotropic phase, where one expects liquidlike behavior, the storage moduli of all samples should be close to 0, that is, undetectable. $G'(T)$ starts to increase strongly at $T \approx (34 \pm 0.5)$ °C, taking values of 10^5−10^6 Pa at 20 °C (see Figure 5B−D). A small increase of the absolute values with particle concentration was observed.

As shown in Figure 6, the absolute values for the moduli may vary by as much as a factor of 4 if the scan is repeated after exchanging sample material. Outside the considerable scatter for results from identical samples, no systematic dependence on particle size was seen within 1 order of magnitude.

The shapes of the temperature spectra are almost independent of particle size and concentration (Figure 5). In all cases, two well-separated slopes exist: a large slope during the first 2−3° after the transformation, followed up by a smaller one for temperatures below ≈31 °C. These intervals can be related to changes of the structure shown in Figure 2. Therefore, we relate the increase of $G'(T)$ to the onset of the transition, T_{IN}. Network formation, however, may set in slightly below T_{IN}. At the cooling rates investigated, network formation takes place during the first 1−3° below T_{IN}. During this period the network walls show marked rearrangements. Only at even lower temperatures rearrangement of walls ceases until hardly any macroscopic changes take place. However, the network

(32) van Blaaderen, A. Private discussions.

(33) Kneppe, H.; Schneider, F.; Sharna, N. K. *Ber. Bunsen-Ges. Phys. Chem.* **1981**, *85*, 784.

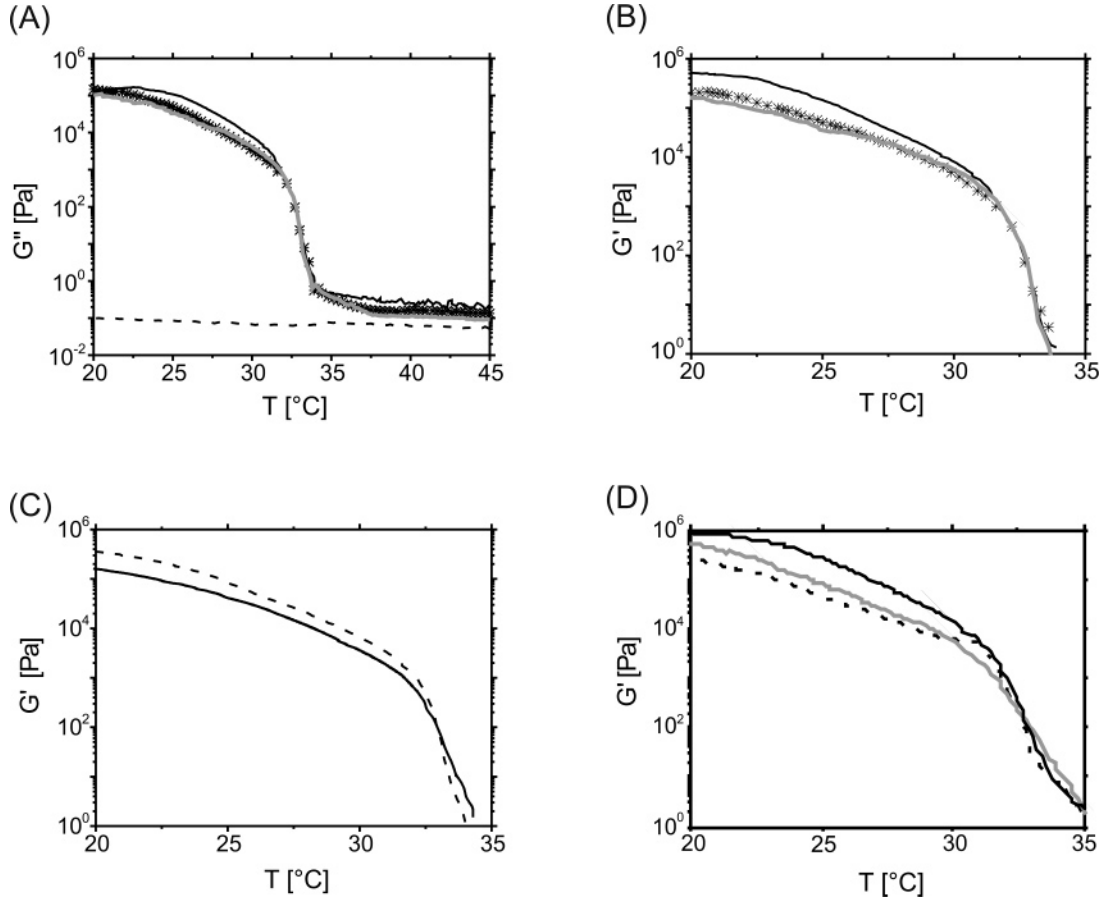

Figure 5. Temperature dependence of (A) the loss (G'') and (B) the storage (G') moduli for suspensions of 10 wt % of sterically stabilized PMMA particles dispersed in 5CB. The shear frequency was kept fixed, $f = 1$ Hz. (*) $R = 120$ nm; (grey line) $R = 370$ nm and (black line) $R = 780$ nm; dashed line, pure 5CB. (C and D) Temperature dependence of the storage modulus (G') for a 5 wt % weight fraction of particles (C) and 15 wt % (D) weight fraction of particles, respectively; (solid line) $R = 120$ nm, (dashed line) $R = 610$ nm, and (grey line, part D only) $R = 100$ nm. For moduli above $\approx 5 \times 10^5$ Pa and below 1 Pa there are systematic errors caused by the resolution of the rheometer, which cannot be quantified.

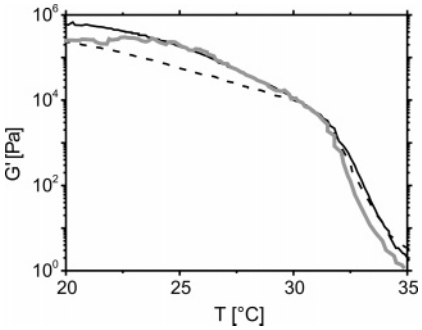

Figure 6. Temperature dependence of the storage G' modulus for three identically treated suspensions of 15 wt % 120-nm-sized sterically stabilized PMMA particles in 5CB. The three spectra show the reproducibility of the data for successive loadings of the rheometer. The samples cooled from 45 to 15 °C at a rate of −10 K/h. The shear frequency was constant at $f =$ 1 Hz.

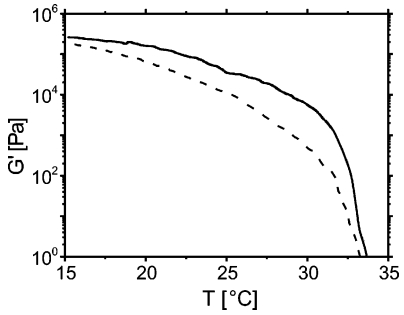

Figure 7. Temperature dependence of the storage modulus $G'(T)$. A total of 10 wt % of 370-nm-sized particles are dispersed in 5CB. The dashed line shows the spectrum of a sample after addition of another 2 wt % of hexane, whereas no hexane was added to the sample belonging to the solid line. Both samples were cooled from 45 to 15 °C with −10 K/h. The shear frequency was constant at $f = 1$ Hz.

may still consolidate (Figure 2), in agreement with a further increase of the fraction of nematic material; see Figure 4.

Because the width of the biphasic region increases with hexane concentration (see Figure 3), we were prompted to ask whether this has an influence on the mechanical properties of the network. Figure 7 shows $G'(T)$, $f = 1$ Hz, for a suspension containing 10 wt % of 370-nm-sized particles dispersed in 5CB before (solid line) and after (dashed line) addition of another 2 wt % of hexane. Strikingly, the values for $G'(T)$ are by up to a factor of 8 smaller than for the sample without hexane added and the strong increase of $G'(T)$ after passing the phase transformation is smeared out. However, close to 15 °C the difference in $G'(T)$ between both samples has decreased toward a factor of 2. The smaller slope between 25 and 35 °C was beyond the scatter range observed in reloaded samples. The decrease of T_{IN} is less than expected for binary mixtures of hexane and 5CB, according to eq 1. Whereas the addition of 2 wt % hexane is expected to cause a decrease of T_{IN} by an additional 8°, a decrease of only ≈1 °C was found in Figure 7. On the other hand, the

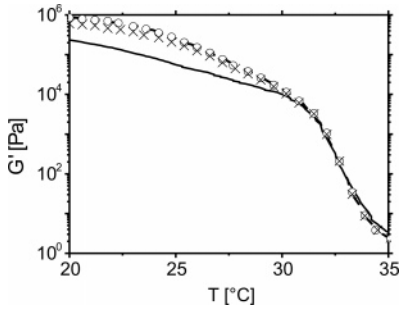

Figure 8. Temperature dependence of the storage modulus $G'(T)$ for a suspension containing 15 wt % of 120-nm-sized PMMA particles dispersed in 5CB. The sample was taken five times through a cooling/heating cycle, with upper and lower temperature limits at 45 and 15 °C, respectively. Only the cooling scans are shown. The sample was not sheared between successive runs. (Black solid line, first cooling; dashed line, second cooling; ○, third cooling; ×, fifth cooling.) Typically, the time lag between two successive scans was on the order of a few minutes. Only after the fourth cooling the sample was left to 15 °C overnight. Cooling rate, −10 K/h; heating rate, 15 K/h. The shear frequency was kept constant at $f = 1$ Hz.

intensively dried samples remained liquidlike after homogenizing for 1 week. The storage modulus of these samples could not be determined with the present setup. This indicates that the remaining amounts of hexane do not sufficiently slow the growth rate of nematic domains sufficiently, so that the particles were overtaken by the isotropic/nematic interface before network structures could be formed.

IV. Reversibility of Network Formation

A. Rheology. We also wanted to test if the changes of the storage modulus are reversible during repeated cooling and heating of a sample without changing the sample material. Figure 8 shows an example of a sample containing 15 wt % of 120-nm-sized particles taken through five cooling and heating cycles, $f = 1$ Hz. Only the cooling runs are shown. After passing the isotropic-to-nematic transformation, an increase of the storage modulus by several orders of magnitude was observed. Interestingly, the second and successive cooling runs resulted in even higher storage moduli for temperatures below ≈30 °C. The increase of the storage modulus suggests that taking a sample through several cooling/heating cycles results in strengthening of the network.

B. Microcalorimetry. A difference between the first and successive coolings may also be observed in the specific heat. Figure 9 shows the thermograms of three samples taken through a cooling/heating cycle up to 13 times. The samples differed in the period of homogenization, which influences the amount of liberated hexane (see Figure 3B). The more hexane is set free, the lower T_{IN} was measured as compared to pure 5CB ($T_{IN}^{5CB} = 35.2$ °C). For the first cooling, the first sample showed a reduction of T_{IN} by 0.4 °C (see Figure 9A), for the second sample by 0.7 °C (see Figure 9B), and for the third sample by 2.6 °C (see Figure 9C). According to eq 1 the biphasic region was entered at a concentration of 0.1 wt % hexane for the first sample, 0.18 wt % for the second sample, and 0.65 wt % for the third sample.

Independent of the reduction of T_{IN}, during the first cooling $C_v^{rel}(T)$ always showed a single peak; see Figure 9. In case of a minor reduction of T_{IN}, that is, for low hexane concentrations, the thermograms remained almost identical, even if the sample was taken through 11 cooling and heating cycles; Figure 9A.

For larger reduction of T_{IN} a splitting of the peak in $C_v^{rel}(T)$ may be observed. If the peak splits, the first peak shows a decrease in the values of $C_v^{rel}(T)$ and temperature as more cycles are completed and the second an increase in both. This diverging behavior is consistent with the invariance of total heat of the phase transformation. Given that a peak in the specific heat corresponds to a phase transformation, a splitting of the peak suggests the coexistence of two well-separated regions, where the liquid crystal passes its isotropic−nematic phase transformation at different temperatures.

A splitting of the peak is observed after eight cycles in Figure 9B. The splitting becomes increasingly pronounced for further cycles. The squares in Figure 9B denote the 13th cooling and heating cycle. Taking the temperature at the peak maxima as the phase transition temperature (eq 1), after 13 cycles the average hexane concentrations are estimated to be 0.25 wt % at the maximum of the first ($T = 34.2$ °C) and 0.15 wt % at the maximum of the second peaks ($T = 34.6$ °C). Note that in the particle-rich domains the average hexane concentration may be much higher. For large reductions of T_{IN} (in case of the third sample T_{IN} is reduced by 2.6 °C compared to pure 5CB), that is, high hexane concentrations, a splitting of the peak was already observed for the second cooling, Figure 9C. In this case a more pronounced separation of the peak maxima was observed, most likely caused by stronger variations of the position-dependent hexane concentration. According to eq 1 the hexane concentrations belonging to the maxima of both peaks already differ by ≈0.2 wt % after four cooling/heating cycles.

C. LSCM. To gain complementary information on the reason of peak splitting and increase of $G'(T)$ for successive cooling and heating runs, we investigated a sample by LSCM. Figure 10 shows the influence of the temperature and of successive cooling and heating cycles on the structure of the sample. The suspension was cooled with a constant rate of −6 K/h from 12 K above the phase transition $T_{IN} = 33.3$ °C down to 25 °C and left for 19 h. The next day, the suspension was reheated to 45 °C with a constant rate of 6 K/h. The sample was taken through this cooling/heating cycle twice more.

The first cooling was discussed in section III.B. An 80 μm × 80 μm sized image of the structure in the nematic is shown in Figure 10A (see also Figure 2H). After 19 h at 25 °C (Figure 10B) and even during reheating to T_{IN}, the structure hardly changed. Above T_{IN} particles and particle clusters slowly broke off the network, Figure 10C. Even 2 h after passing T_{IN} significant parts of the particle walls still existed (Figure 10D), although particle-free domains were no longer visible. After the start of a second cooling cycle the breaking up of the network proceeded as long as $T > T_{IN}$. Nematic domains were visible at 33.82 °C, a temperature 0.6 K higher than during the first cooling. Figure 10E shows the structure just above T_{IN} ($T = 33.94$ °C). The sample appeared almost homogeneous, although still darker regions could be resolved. Passing T_{IN}, the network formed very rapidly and little macroscopic rearrangement occurred below T_{IN}; see Figure 10G,H. These observations point toward a memory of the preexisting structure. The memory depends on the time span the system was tempered in the isotropic phase and may also be influenced by wall effects. Furthermore, it seems to depend on hexane concentration, that is, on reduction of T_{IN}. In ref 34 it has been shown that for higher hexane concentration, that is, lower T_{IN}, the walls may remain

(34) Vollmer, D.; Schofield, A. B.; Hinze, G. *Prog. Colloid Polym. Sci.* **2004**, *129*, 1.

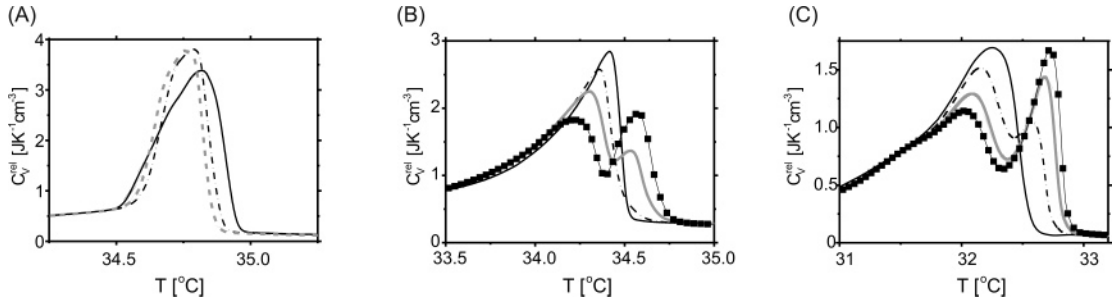

Figure 9. (A) Dependence of the specific heat C_v^{rel} on temperature for a mixture of 5 wt % PMMA particles ($R = 370$ nm) dispersed in 5CB. The sample was taken through 11 cooling (cooling rate, −5.9 K/h) and heating (heating rate, 6.7 K/h) cycles. Upper temperature, 40 °C; lower temperature, 25 °C. (Solid line, 1st cooling; dashed line, 3rd cooling; gray line, 11th cooling,) (B) Dependence of the specific heat C_v^{rel} on temperature for a mixture of 5 wt % PMMA particles ($R = 120$ nm) dispersed in 5CB. The sample was taken through 13 cooling (cooling rate, − 6.2 K/h) and heating (heating rate, 90 K/h) cycles. Upper temperature, 50 °C; lower temperature, 25 °C. (Solid line, 1st cooling; dashed line, 5th cooling; gray line, 8th cooling; square, 13th cooling.) (C) Dependence of the specific heat C_v^{rel} on temperature for a mixture of 10 wt % PMMA particle ($R = 430$ nm) dispersed in a mixture of 5CB. The sample was taken through four cooling (cooling rate, −4.5 K/h) and heating (heating rate, 4.8 K/h) cycles. Upper temperature, 45 °C; lower temperature, 1 °C. (Solid line, 1st cooling; dashed line, 2nd cooling; gray line, 3rd cooling; square, 4th cooling). Always, the maximum temperature and the minimum temperature were held for about 5 min before starting the next temperature run.

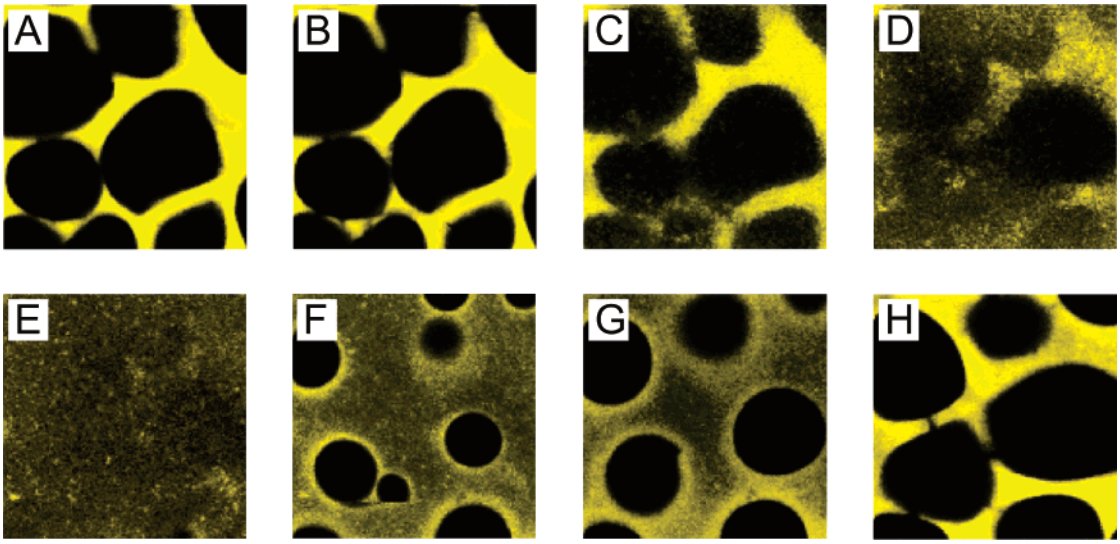

Figure 10. Images of a sample containing 15 wt % fluorescently labeled PMMA particles ($R = 204$ nm) dispersed in a mixture of 5CB. Images of the first cooling are shown in Figure 2. The sample was taken twice through a cooling/heating cycle. (A) 25.0 °C; (B) 25.0 °C; (C) 38.61 °C; (D) 41.13 °C; (E) 33.94 °C; (F) 33.82 °C; (G) 33.70 °C; (H) 27.35 °C. Part A images the sample after the first cooling cycle, and part B images the sample after leaving the sample for 22 h at 25 °C. Cooling rate, −6 K/h; heating rate, 6 K/h. Confocal area: 80×80 μm^2. Images were taken 10 μm beyond the coverslip.

fairly intact even after 4 h in the isotropic phase. The reduction of particle movement after repeated cooling points toward a stronger binding of the particles in the walls, consistent with the higher elastic moduli (Figure 8). No signs of sedimentation were detected on the time scale investigated as close as 10 μm to the bottom of the sample, where the image plane was chosen.

V. Discussion and Conclusions

Network formation can be regarded as a result of phase separation on the micrometer scale, with colloids being expelled from the nematic phase. It is driven by orientational elasticity of the nematic phase, anchoring energy, and surface tension at the liquid crystal/particle interface.[18,29] Because anchoring energy depends on particle size, the latter should also be expected to contribute to particle rearrangement. Surprisingly, in particles of different sizes we found networks of similar shape and similar dynamics of formation as shown by LSCM and rheology, although size trends could be masked by poor reproducibility as shown in Figure 6. These observations suggest that forces independent of particle size are crucial for particle movement and rearrangement in networks. In mixtures with PMMA particles, we found that the kinetics of phase transition was altered. As indicated both by calorimetry and NMR spectroscopy, the temperature and time intervals of phase transformation are broadened. Within this interval isotropic and nematic domains coexist. Moreover, we have shown that network formation as well as calorimetric changes are strongly influenced by pretreatment of the particles. This indicates that most likely the presence of a third component that alters phase transition kinetics is a key factor in network formation. PMMA particles are prepared by emulsion polymerization and stored in alkane solvents (in our case, hexane) for up to several years. During this period, alkanes can penetrate even into the core of the colloids. Depending on temperature and vacuum pressure, prolonged drying may cause evaporation of the fraction of alkane located within the poly-12-hydroxy-stearic acid stabilization layer and the outermost part of the colloids, whereas the alkane remnants trapped within the core are very difficult to remove. During subsequent homogenization, residual alkane is slowly liberated, which explains the long

homogenization periods required for the detection of phase transformation changes. We have shown that very small amounts of hexane, which is miscible with 5CB at all temperatures observed (boiling point = 69 °C), result in optically discernible coexisting isotropic and nematic domains within the phase transformation interval whose interfaces move slowly enough to be observed microscopically. The growth rate of the nematic domains and, thus, the speed of the moving nematic front at a defined cooling rate depend on the hexane concentration in bulk liquid crystal. It is to be expected that additives other than hexane, e.g., alkanes of higher chain length or cyclic organic solvents, exert similar effects depending on size, polarity, and steric conformation. Preliminary studies (data not shown) revealed that particles remain in the isotropic domain and are moved ahead of the isotropic/nematic interface within a broad range of interface velocities until shrinking of the isotropic domains leads to confinement and steric hindrance. That the effect of hexane concentration on network formation is independent of colloid size hints that hexane predominantly affects size-independent parameters.

By NMR spectroscopy, we found that substantial amounts of isotropic material are present even at temperatures as much as 10 K below T_{IN} of pure 5CB, Figure 4, where the resolution of calorimetry is not sufficient. In previous studies, it was argued that suppression of the isotropic/nematic phase transition until several Kelvin below the expected T_{IN} could be caused by distortions of the director field at the particle surface.[16] According to our findings this is unlikely, because the shift of the transformation temperature depends on the period of homogenization whereas the number of particles remains constant. On the other hand, anchoring of the director on the particle surface could be altered by clustering and confinement of the particles or by wetting with isotropic material and/or low-molecular-weight impurities such as alkane. In ref 17, the authors assumed that the particles are embedded in isotropic material and that network formation is associated with suppression of the nematic phase due to confinement.[35] In our preparations, however, we found no evidence for confinement-induced suppression of the phase transformation as no significant differences could be detected in network morphology and calorimetric parameters between smaller and larger particles. In micrometer-sized particles, the width of the spaces between the particles in the network is about 2 orders of magnitude larger than the nematic correlation length of 10 nm determined for 5CB.[16] Because of the large distance between the colloids it is unlikely that the colloids themselves could alter the phase transition temperature and kinetics of bulk 5CB.

As in previous studies,[14,15,35] we found an increase of the storage modulus (Figure 5), when cooling through the phase transformation. At temperatures just below T_{IN}, a sharp increase of $G'(T)$ was observed, followed by a slower increase at temperatures well below T_{IN}. The corresponding temperature intervals are in accordance with the NMR results. This suggests that both network formation and stabilization essentially take place within the biphasic interval. Further compaction of the network as indicated by a further increase of $G'(T)$ at temperatures far below T_{IN} could be explained by NMR data showing that even then the phase transformation is still incomplete (Figure 4). For particle sizes $0.1\ \mu m < R < 1\ \mu m$, the temperature dependence of the storage moduli did not differ significantly, Figure 5, in line with our observation that network morphology also does not strongly depend on particle size. This is in contrast to the findings of Petrov et al.,[35] who proposed a particle size dependence of the storage modulus $G'(R_1)/G'(R_2) \sim (R_2/R_1)^2$. For our $R_1 = 100$ nm and $R_2 = 780$ nm sized particles, this predicts $G'(R_1)/G'(R_2) \approx 60$, which is incompatible with our findings shown in Figure 5. Those authors found the storage moduli to be *lower* for suspensions with $R = 100$ nm particles than those for larger particles by 3 to 4 orders of magnitude. Hence, they suggested that network formation could be suppressed in small particles. We occasionally observed similar curves; however, these were not reproducible and could be caused by artifacts (see the appendix).

Studies on repeatedly cooled and reheated 5CB/PMMA particle mixtures provided an important insight into the mechanism by which the phase transformation interval is altered and, thus, into the origin of network formation. We found that, after repeated cooling, the slow increase of G' at lower temperatures was enhanced, indicating further compaction of the network with every cycle (Figure 8). This was accompanied by an increasingly slow dissolution of the network upon reheating and increasing memory effects upon re-forming of the structure during re-cooling as visualized by LSCM (Figure 10). Annealing and reorganization of particles within the network probably leads to a shrinking average distance between particles and to enhanced van der Waals attraction. Calorimetry revealed that the temperature dependence of $C_v^{rel}(T)$ changed with repeated re-forming of the network until two separate heat peaks, a broad one at lower and a sharp one at higher temperatures, emerged (Figure 9). Given that a peak in specific heat represents a phase transformation, the presence of two separate peaks points to the coexistence of two distinct compartments where the liquid crystal becomes nematic at different temperatures.

As concluded from the optical findings (Figure 1), obviously the liquid crystal compartment with the lower phase transformation temperature must be located in the network walls. The difference in concentration of hexane between both compartments depends on sample preparation and especially on the number of heating and cooling cycles. Differences of up to 0.2 wt % hexane between both compartments were established after four cycles (see Figure 9C, eq 1). After long periods (i.e., weeks) in the isotropic phase, these local concentration differences will probably disappear. However, as long as there is a local enrichment of particles, inhomogeneities in the alkane concentration will persist and vice versa. It remains to be elucidated if this mechanism is unique to PMMA particles or if it is relevant in other colloid types as well.

It has been reported previously[35] that in mixtures of liquid crystals and colloids, the heat peak can be split even during the first cooling. This was attributed to two sequential first-order phase transitions in the liquid crystalline matrix: First, particle-rich domains assemble that later collapse into self-supporting networks. However, our calorimetric results contradict this hypothesis. We never observed peak splitting at the first cooling (see Figures 3 and 9). Also, the NMR results do not provide any hint toward a second phase transition (Figure 4). Rather, a gradual decrease in the amount of isotropic material is observed. It should be noted that the authors of ref 35 used different equipment.[36]

(35) Petrov, P. G.; Terentjev, E. M. *Langmuir* **2002**, *17*, 2942.

(36) According to our experience, in a Perkin-Elmer calorimeter (used in ref 35) it is hard to keep the sample isotropic during loading. The second peak, therefore, may have been caused by a temperature drop during the loading procedure.

Taken together, we have shown that phase-transformation-induced particle movement and network formation take place in 5CB−PMMA mixtures for a wide range of compositions and preparation procedures. Whereas both have proven to be quite insensitive to particle concentration and size (and, thus, to the anchoring energy), broadening of the temperature interval of phase transformation and coexistence of isotropic and nematic domains during this interval have been identified as crucial factors. As shown by repeated heating and cooling, enrichment of particles in the network walls is associated with the formation of two separate compartments of liquid crystal that become nematic at different temperatures. This phenomenon is consistent with slow liberation and redistribution of alkane originating from particle synthesis. These are enriched in the vicinity of the particles and eventually in the network walls. This mechanism confers high stability and strong memory effects to the network.

Acknowledgment. The authors thank Günter Auernhammer, Julie Cleaver, Franck Clement, Jason Crain, Harald Pleiner, Sara Romer, Holger Stark, and Jürgen Vollmer for stimulating discussions. Thomas Basché is gratefully acknowledged for making the confocal microscope available. D.V. acknowledges funding by the European Commission under the Marie Curie program and by LEA. A.B.S. is supported by the NASA Microgravity Sciences Program.

Appendix

In this appendix we would like to discuss some artifacts frequently encountered in rheological measurements. Examples of curves representing typical artifacts are given in Figure 11. The spectra correspond to measurements using a high strain amplitude (i), a high frequency (ii), a high cooling rate (iii), and a high cooling rate plus a low alkane concentration (iv). Spectrum (v) shows a typical example of a measurement where the reason of the obvious irregularity could not be identified.

As a rule we observed that the values for the storage modulus were especially sensitive to the choice of the parameters during the temperature interval of network formation. As shown in Figure 2, during this period the movement of the particles is fast and, even after their motion has almost ceased, the particle walls may rearrange. During this period, the structure is fragile and a high strain [Figure 11(i)] may break up the percolating network walls, leading to a much lower storage modulus. In contrast, a high frequency [in this case 10 Hz, Figure 11(ii, dashed line)] after an initial increase typically causes

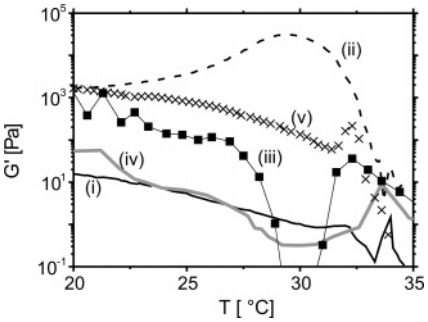

Figure 11. Examples of the temperature-dependent storage modulus, $G'(T)$. All particles were dispersed in 5CB, and no extra hexane was added. (i, black line) Particle concentration, 5 wt %; size, $R = 240$ nm; cooling rate, −30 K/h; strain amplitude, 10%; shear frequency, 1 Hz; (ii, dashed line) particle concentration, 10 wt %; size, $R = 460$ nm; cooling rate, −4 K/h; strain amplitude, 1%; shear frequency, 10 Hz; (iii, squares, solid line) particle concentration, 10 wt %; size, $R = 240$ nm; cooling rate, −60 K/h; strain amplitude, 1%; shear frequency, 1 Hz; (iv, gray line) particle concentration, 5 wt %; size, $R = 240$ nm; cooling rate, −100 K/h; strain amplitude, 1%; shear frequency, 1 Hz; the sample was measured 1 week after preparation; (v, crosses) particle concentration, 10 wt %; size, $R = 240$ nm; cooling rate, −15 K/h; strain amplitude, 1%; shear frequency, 1 Hz.

a decrease of $G'(T)$ possibly due to slippage of the sample at the cone or plane. Small amounts of liquid crystal expelled from the network could be sufficient to reduce $G'(T)$ significantly. Typically, the storage moduli decrease with increasing cooling rate. Especially with cooling rates of more than ≈−60 K/h we observed that, after the onset of network formation, that is, after an initial increase, $G'(T)$ decreased by orders of magnitude, sometimes followed by another increase; see spectrum iii (squares). This phenomenon was enhanced if the sample was measured shortly after preparation (iv, gray line). If the biphasic region is not sufficiently broad the time interval is not long enough for particles to arrange in stable networks. The time span of network formation decreases with higher cooling rates and lower alkane concentrations. Presumably this results in a less compact structure and, thus, in lower values for the storage modulus. Spectrum Figure 11(v) is characterized by a peak shortly after the initial increase of the storage modulus. In such cases, $G'(T)$ may increase again under further cooling or decrease even further. This could be explained by slippage leading to partial detachment of the sample from the walls. In poorly reproducible spectra a peak always occurred in combination with lower values for $G'(T)$ compared to normal spectra.

LA047090W